Supplementary Information

Use of ATR-FTIR with D/H Substitution for Assessing Water Uptake in Alkali Perchlorate Matrices

*Mohammed Alfatih Hamid, Ezgi Kutbay, Sefik Suzer**
Bilkent University, Faculty of Science, Department of Chemistry, Cankaya, 06800 Ankara, Turkey
Corresponding author*, e-mail address: suzer@fen.bilkent.edu.tr

Additional experimental XPS and XRD data, along with detailed theoretical vibrational analyses (F-G matrix formalism and harmonic-oscillator calculations), are provided to support the spectroscopic interpretations discussed in the main manuscript.

S1. Additional experimental data

Figure S1 presents the XPS spectra of the $KClO_4$–$LiClO_4$ mixture. Signals from Cl 2p, K 2p, Li 1s, and O 1s are all identified, confirming that both salts are present in the analyzed specimen.

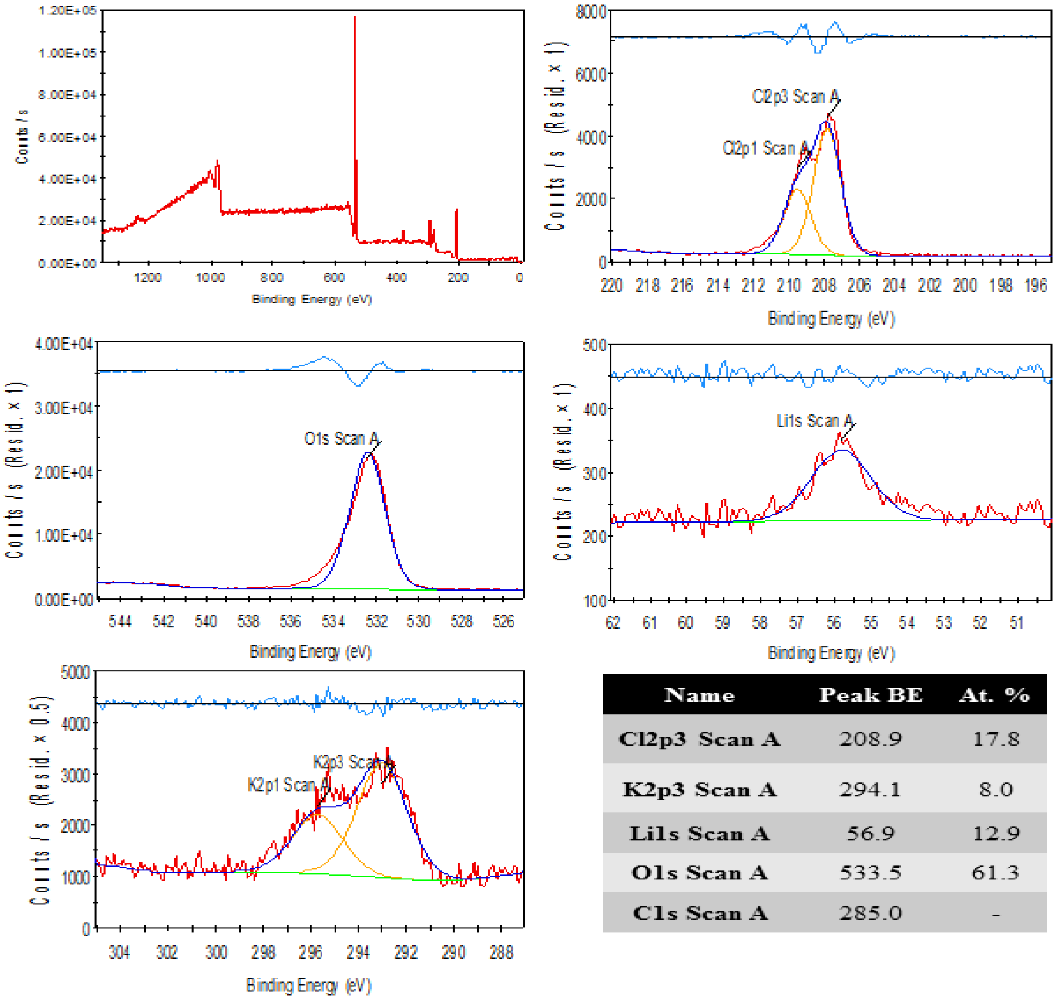

Name	Peak BE	At. %
Cl2p3 Scan A	208.9	17.8
K2p3 Scan A	294.1	8.0
Li1s Scan A	56.9	12.9
O1s Scan A	533.5	61.3
C1s Scan A	285.0	-

Figure S.1. XPS analysis confirming the presence of $KClO_4$ in binary mixtures.

In particular, the K 2p doublet corresponds to an atomic fraction of ~8%, demonstrating that $KClO_4$ is physically incorporated into the mixture. This complements the ATR-FTIR results in the main manuscript, where no K-associated vibrational features were detected. The combined data show that while $KClO_4$ is present in the solid matrix, it does not participate in water uptake under the conditions examined.

Figure S2 shows the XRD patterns of $LiClO_4$, $NaClO_4$, and $KClO_4$ alongside their corresponding ICDD reference data. $LiClO_4$ and $NaClO_4$ match the reflections of their known hydrated phases ($LiClO_4 \cdot 3H_2O$ and $NaClO_4 \cdot H_2O$), whereas $KClO_4$ aligns with its anhydrous structure. These patterns confirm the phase identity of the salts as used in the study and provide structural support for the hydration behavior discussed in the main manuscript.

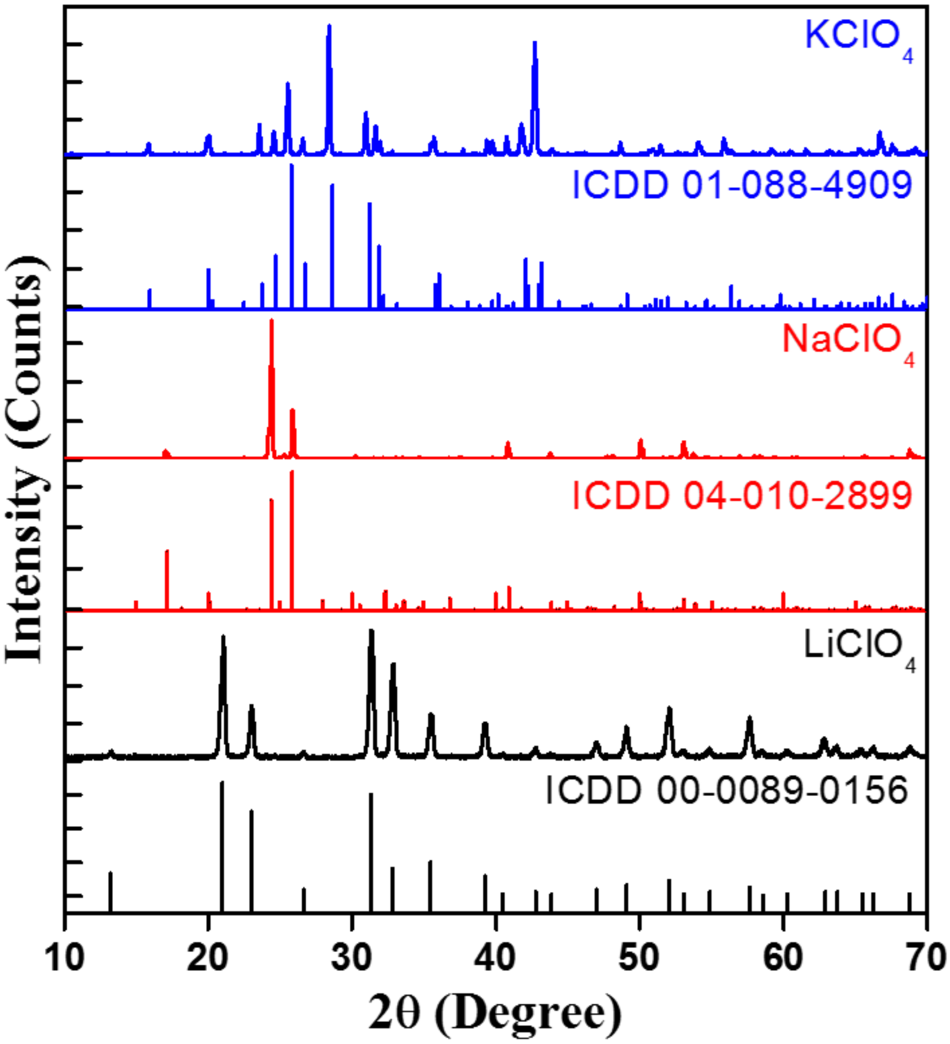

Figure S. 2. XRD patterns of $LiClO_4$, $NaClO_4$, and $KClO_4$ samples compared with reference ICDD data.

Figure S3 compares the XRD patterns of the pure perchlorate salts with those of the ternary Li–Na–K mixtures prepared by solution and mechanical routes. Both ternary samples display superimposed reflections that correspond to $LiClO_4$, $NaClO_4$, and $KClO_4$, with no additional peaks indicating new phase formation. These structural data complement the ATR-FTIR results in the main manuscript by confirming that the ternary system remains a combination of the parent salts, with hydration behavior dominated by Li^+ environments.

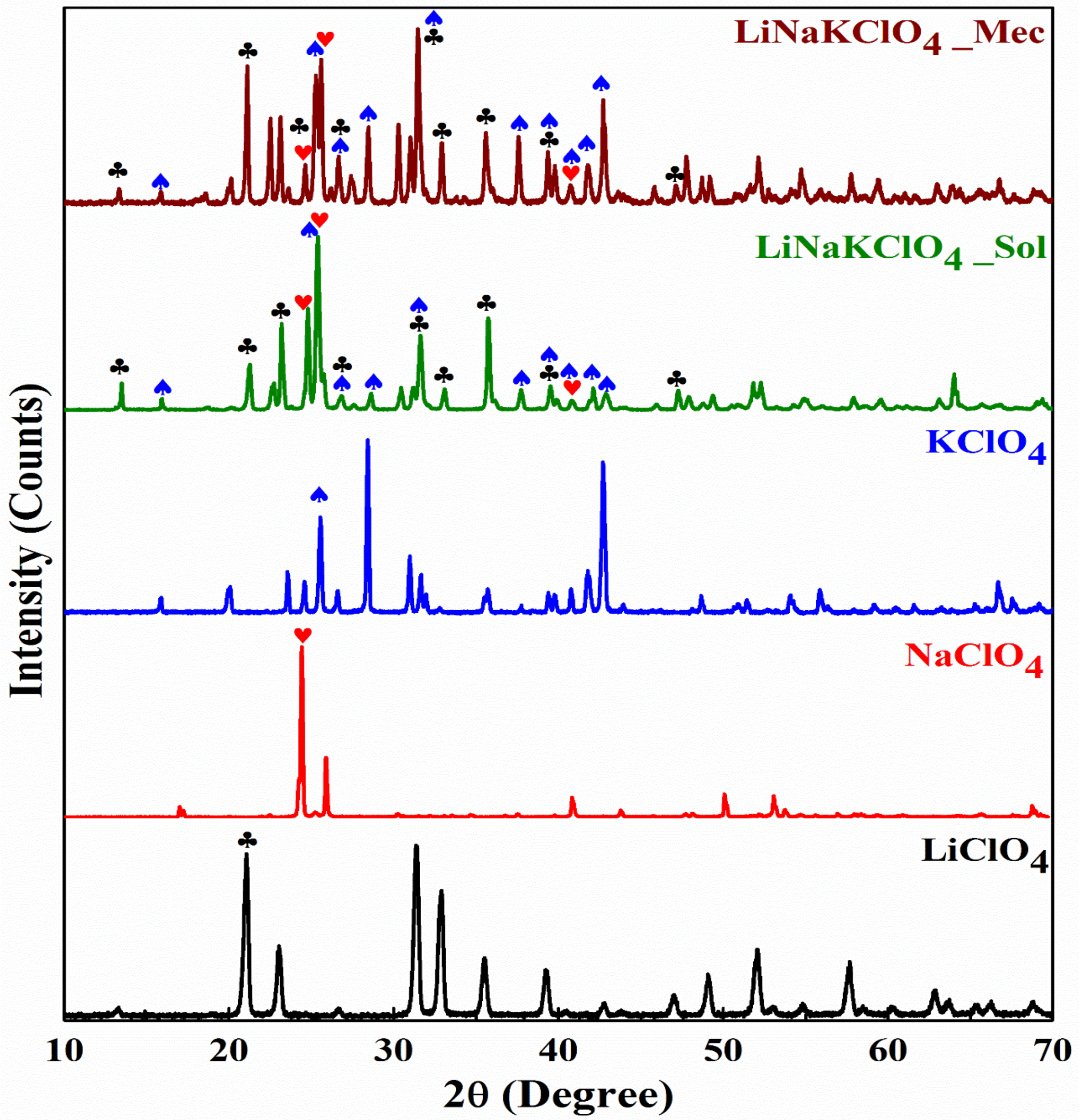

Figure S. 3. Powder XRD patterns of pure $LiClO_4$, $NaClO_4$, and $KClO_4$ salts, together with the ternary Li–Na–K perchlorate mixture prepared via solution-based (green) and mechanical grinding (brown) routes. Phase attribution markers indicate reflections corresponding to $LiClO_4$ (♣), $NaClO_4$ (♥), and $KClO_4$ (♠).

S.2. Theoretical Analysis

S.2.1. Wilson F-G Matrix Analysis of Vibrational Mode

To analyze vibrational mode behavior in confined environments, we employ Wilson's GF matrix method to decompose the observed frequencies of H_2O and D_2O in $LiClO_4$ and $NaClO_4$ matrices into geometric and mechanical contributions. This approach involves solving the secular equation:

$$| FG - \lambda I | = 0$$

where the eigenvalues λ_i are related to the vibrational frequencies ν_i via:

$$\lambda_i = 4\pi^2 c^2 \nu_i^2 \approx \mathrm{F}_i \mathrm{G}_i$$

Here, **F** is the force constant matrix, and **G** is the inverse kinetic energy matrix, which depends on atomic masses and molecular geometry. For the stretching modes of water in a bent XY_2 configuration, the vibrational eigenvalues simplify to:
For symmetric stretch (ν_1):

$$\lambda_1 = F_{11}G_{11} = (f_r + f_{rr}) \cdot G_{11}$$

For antisymmetric stretch (ν_3):

$$\lambda_3 = F_{33}G_{33} = (f_r - f_{rr}) \cdot G_{33}$$

Taking their ratio yields:

$$\frac{\nu_3}{\nu_1} = \sqrt{\frac{\lambda_3}{\lambda_1}} = \sqrt{\frac{(f_r - f_{rr})}{(f_r + f_{rr})}} \cdot \sqrt{\frac{G_{33}}{G_{11}}}$$

For a non-linear triatomic molecule like H_2O, the G-matrix diagonal elements are expressed as:

$$G_{11} = \mu_Y + \mu_x(1 + \cos\alpha)$$

$$G_{33} = \mu_Y + \mu_x(1 - \cos\alpha)$$

where μ_Y and μ_x are the reciprocal masses of the terminal (H or D) and central (O) atoms, respectively, and α is the H–O–H bond angle. For $LiClO_4$, a reduced bond angle of 103° is used, based on structural characterization of $LiClO_4 \cdot H_2O$.[1] Since the $NaClO_4$ environment more closely resembles isolated water molecules, the standard gas-phase H–O–H angle of 104.5° is applied.

We first calculate the geometric factors $\sqrt{(G_{33}/G_{11})}$ from the bond angles (103° for $LiClO_4$, 104.5° for $NaClO_4$) and atomic masses. Using these geometric factors along with the experimentally determined H_2O vibrational frequencies ($LiClO_4$: $\nu_1 = 3523$, $\nu_3 = 3563$ cm^{-1};

$NaClO_4$: ν_1 = 3535, ν_3 = 3585 cm^{-1}), we extract the force constant ratios $\sqrt{((f_r\text{-}f_{rr})/(f_r\text{+}f_{rr}))}$ from the experimental frequency ratios using the above expression. The key assumption is that the electronic environment (and thus force constants) remains the same when H is replaced by D. Therefore, the force constant ratios determined from H_2O apply directly to D_2O in the same salt matrices. For D_2O, we recalculate the geometric factors using deuterium mass (m_D = 2) instead of hydrogen (m_H = 1), while keeping the same bond angles. Combined with the unchanged force constant ratios, this predicts the D_2O frequency ratios, which can be validated against experimental data (ν_3 = 2653 cm^{-1} for $LiClO_4$ and 2668 cm^{-1} for $NaClO_4$).

The results of this analysis are summarized in the **Table S1**, which shows the complete decomposition of frequency ratios into geometric and force constant contributions for both H_2O and D_2O systems:

Table S1. Vibrational frequency analysis of H_2O and D_2O in $LiClO_4$ and $NaClO_4$ salt matrices using Wilson's GF matrix method

Salt	**Molecule**	**ν_1 (cm^{-1})**	**ν_3 (cm^{-1})**	**ν_3/ν_1**	$\sqrt{\frac{G_{33}}{G_{11}}}$	$\sqrt{\frac{(f_r - f_{rr})}{(f_r + f_{rr})}}$	**$\Delta\nu$ (cm^{-1})**
$LiClO_4$	H_2O	3523	3563	1.01135	1.01332	0.99806	40
$NaClO_4$		3535	3585	1.01414	1.01484	0.99931	50
$LiClO_4$	D_2O	**2593***	2653	**1.02333***	1.02532	0.99806	**60**
$NaClO_4$		**2596***	2668	**1.02757***	1.02830	0.99931	**72**

*Predicted values using experimental ν_3 = 2653 cm^{-1} ($LiClO_4$) and 2668 cm^{-1} ($NaClO_4$)

For D_2O, the enhanced geometric contributions ($\sqrt{(G_{33}/G_{11})} \approx$ 1.025-1.028) compared to H_2O ($\approx$ 1.013-1.015) demonstrate the amplified isotope effect on vibrational coupling. This isotope effect is also evident in the frequency separations $\Delta\nu$, which increase from 40-50 cm^{-1} for H_2O to 60-72 cm^{-1} for D_2O, with $NaClO_4$ consistently showing larger separations than $LiClO_4$ for both isotopes.

Wilson's GF matrix method effectively separates vibrational frequency ratios into geometric and force constant contributions. The analysis reveals that geometric effects play a more significant role in frequency differences, and these effects are further amplified by isotope substitution. The methodology reproduces the general trend in D_2O vibrational frequencies, showing reasonable agreement with experimental data. It also clarifies how different salt matrix environments affect water vibrational behavior, with $NaClO_4$ consistently exhibiting larger frequency separations than $LiClO_4$ for both H_2O and D_2O.

S.2.2. Harmonic Oscillator-Based Estimation of Vibrational Frequencies

To complement the Wilson GF matrix-based vibrational analysis, we additionally apply the harmonic oscillator model to estimate isotopic shifts in vibrational frequencies. The vibrational frequency $\boldsymbol{\nu}$ of a diatomic bond in the harmonic approximation is given by:

$$\tilde{\nu} = \frac{1}{2\pi c}\sqrt{\frac{k}{\mathrm{\mu}}}$$

where $\boldsymbol{k}$ is the force constant (assumed constant for isotopologues in the same chemical environment), $\boldsymbol{c}$ is the speed of light, and μ is the reduced mass of the vibrating atoms. For water isotopologues, μis primarily influenced by the substitution of H (1.008 u) with D (2.014 u), while the oxygen mass (15.999 u) remains unchanged.

Given that:

$$\mu_{OH} = \frac{m_O m_H}{m_O + m_H} \ , \qquad \mu_{OD} = \frac{m_O m_D}{m_O + m_D}$$

The frequency ratio for an O–D bond relative to an O–H bond is approximated by:

$$\frac{\nu_{OD}}{\nu_{OH}} = \sqrt{\frac{\mu_{OH}}{\mu_{OD}}}$$

This simplified mass-scaling relation enables us to predict the fundamental stretching and bending frequencies of D_2O from the experimental values of H_2O. Assuming unchanged force constants between isotopologues, the predicted D_2O frequencies in each salt matrix are computed by applying the reduced mass scaling:

$$\nu_{\mathrm{D_2O,Pred.}} = \nu_{\mathrm{H_2O,Exp.}} \cdot \sqrt{\frac{\mu_{\mathrm{H_2O}}}{\mu_{\mathrm{D_2O}}}}$$

These theoretical predictions are presented alongside experimental data in **Table S2**. Notably, the stretching mode frequencies of D_2O are lower than those of H_2O, consistent with the larger reduced mass. The percentage deviation between predicted and experimental values is also included to evaluate the accuracy of the harmonic oscillator model.

Table S2. Comparison of Experimental and Harmonic Oscillator-Predicted Vibrational Frequencies for H_2O and D_2O in $LiClO_4$ and $NaClO_4$ Matrices

Salt	Vibrational Mode (ν)	Exp. H_2O	Pred. D_2O* (cm^{-1})	Exp. D_2O	Deviation (%)
$LiClO_4$	ν_3 (asym)	3563	2593	2653	2.3
	ν_1 (sym)	3523	2564	2583	0.7
	$\Delta\nu = \nu_3 - \nu_1$	40	-	70	-
	ν_2 (bend)	1624	1182	1210	2.3
$NaClO_4$	ν_3 (asym)	3585	2609	2668	2.3
	ν_1 (sym)	3535	2573	2588	0.6
	$\Delta\nu = \nu_3 - \nu_1$	50	-	80	-
	ν_2 (bend)	1628	1185	1213	2.3

*D_2O values predicted from H_2O using a 0.728 scaling factor, derived from O–H and O–D reduced mass ratio.

Notably, the harmonic oscillator-based predictions show varying degrees of agreement with experimental D_2O frequencies across different vibrational modes. The deviations are consistently larger for the antisymmetric stretching modeand bending mode, reaching approximately 2.3% for both $LiClO_4$ and $NaClO_4$ matrices, while the deviations for the symmetric stretch remain below 0.7%. This discrepancy likely arises from the intrinsic sensitivity of the ν_3 mode to the local electrostatic environment and vibrational coupling effects, which are not captured by the simplified harmonic approximation. The ν_3 mode involves out-of-phase motion of the two terminal atoms, making it more susceptible to perturbations from ion–dipole interactions and hydrogen bonding, even in weakly coordinating perchlorate matrices.[2,3]

The comparable deviations observed between $LiClO_4$ and $NaClO_4$ systems suggest that the hydration environments in both salts exert similar perturbative influences on the vibrational propertiesof confined water molecules. This is consistent with the known structural characteristics of perchlorate salts, where the ClO_4^- anion does not strongly coordinate with water, and the cation–water interactions primarily govern vibrational behavior. As the harmonic oscillator model assumes identical force constants for isotopologues and neglects anharmonic and coupling effects, the similar deviations in both salts reflect the uniform limitations of the model rather than matrix-specific differences. Ultimately, the symmetric stretching shows better agreement with harmonic predictions, while the antisymmetric stretching mode demonstrates enhanced sensitivity to environmental effects beyond the model's scope.

References

1 S. I. Ivlev and D. V. A. N. B. E. F. Kraus, *Monatshefte für Chemie - Chem. Mon.*, 2016, 279–288.

2 A. Nejad and D. L. Crittenden, *Phys. Chem. Chem. Phys.*, 2020, **22**, 20588–20601.

3 M. K. Roy, M. S. Alam, M. M. Hossain, R. Hossain, M. Ruknozzaman, S. Uddin, M. Mahzabin, A. M. Snigdhow and K. Dhar, *J. Sci. Res.*, 2025, **17**, 561–567.